Supplemental Material

A

CD8+ T Cell Panel			
Antibody	Fluorophore	Clone	Manufacturer
CD45.2	FITC	104	Biolegend
CD8a	PE/Cy7	53-6.7	Biolegend
GZB	PE-Dazzle	QA16A02	Biolegend
EOMES	eFluor660	Dan11mag	ThermoFisher
PD-1	PE	RMP1-14	Biolegend

B

CD4+ T Cell Panel			
Antibody	Fluorophore	Clone	Manufacturer
CD45.2	FITC	104	Biolegend
CD4	PE/Cy7	GK1.5	Biolegend
CD25	APC	3C7	Biolegend
FOXP3	PE	MF-14	Biolegend
CD39	PE-Dazzle	Duha59	Biolegend

C

Checkpoint/Costimulatory Receptor Panel			
Antibody	Fluorophore	Clone	Manufacturer
CD45.2	FITC	104	Biolegend
CD8a	PE/Cy7	53-6.7	Biolegend
CD39	PE	Duha59	Biolegend
CD137	APC	17B5	Biolegend
CTLA-4	PE-Dazzle	UC10-4B9	Biolegend
OX-40	PerCP/Cy5.5	OX-86	Biolegend

D

Antigen Presenting Cell Panel			
Antibody	Fluorophore	Clone	Manufacturer
CD45.2	FITC	104	Biolegend
CD11c	PerCP/Cy5.5	N418	Biolegend
CD8a	PE/Cy7	53-6.7	Biolegend
CD40	PE	3/23	Biolegend
CD80	APC	16-10A1	Biolegend
CD86	PE-Dazzle	GL-1	Biolegend

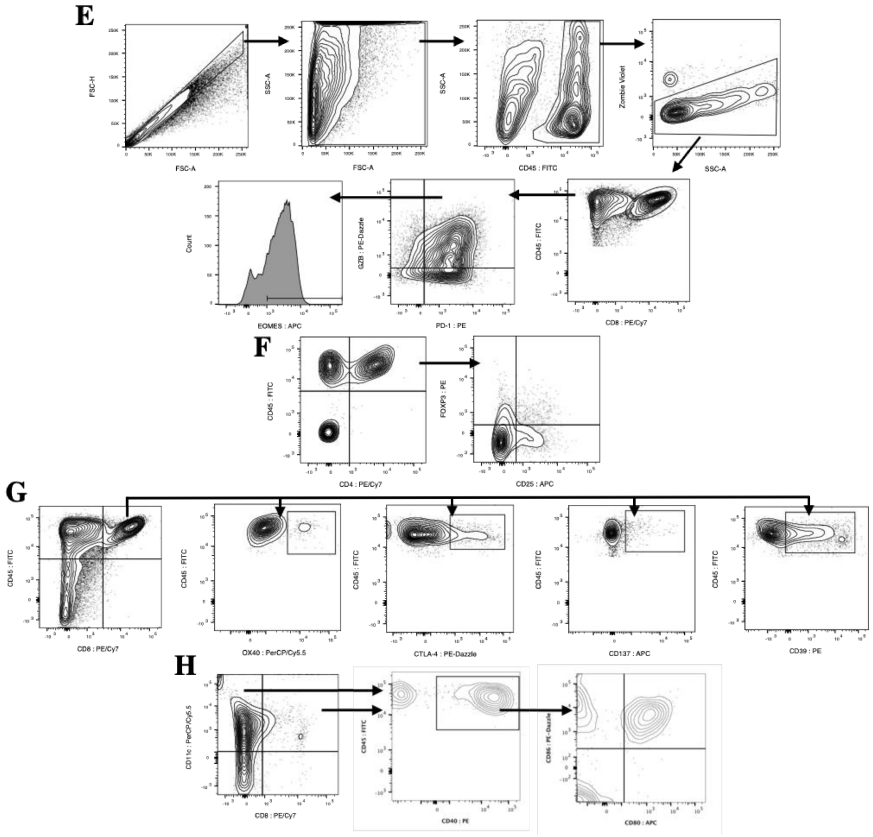

Supplemental Figure S1. Multi-parameter flow cytometry gating strategy. (A-D) Cells were stained with the antibodies and fluorophores listed in the tables and were analyzed on a BD LSRFortessa X20. (E) Singlets were first identified by gating along the 1:1 line of FSC-H vs. FSC-A. Debris was then excluded by gating out small points on the FSC-A axis. Immune cells were selected based on CD45 expression, and live cells were selected based on low uptake of the Zombie Violet stain. $CD8^+$ T cells were gated, and GZB, PD-1, and EOMES expression was quantified in this population. (F) Gating strategy for identifying subpopulations of $CD4^+$ T cells based on expression of CD25, FOXP3, and CD39. (G) Gating strategy for identifying expression of the immune checkpoint CTLA-4, the co-stimulatory receptors CD137 and OX40, and the "immune checkpoint mediator" CD39 on the surface of $CD8^+$ T cells. (H) Gating strategy for identifying $CD11c^+$ dendritic cells and the expression of CD8, CD40, CD80, and CD86 on these cells.

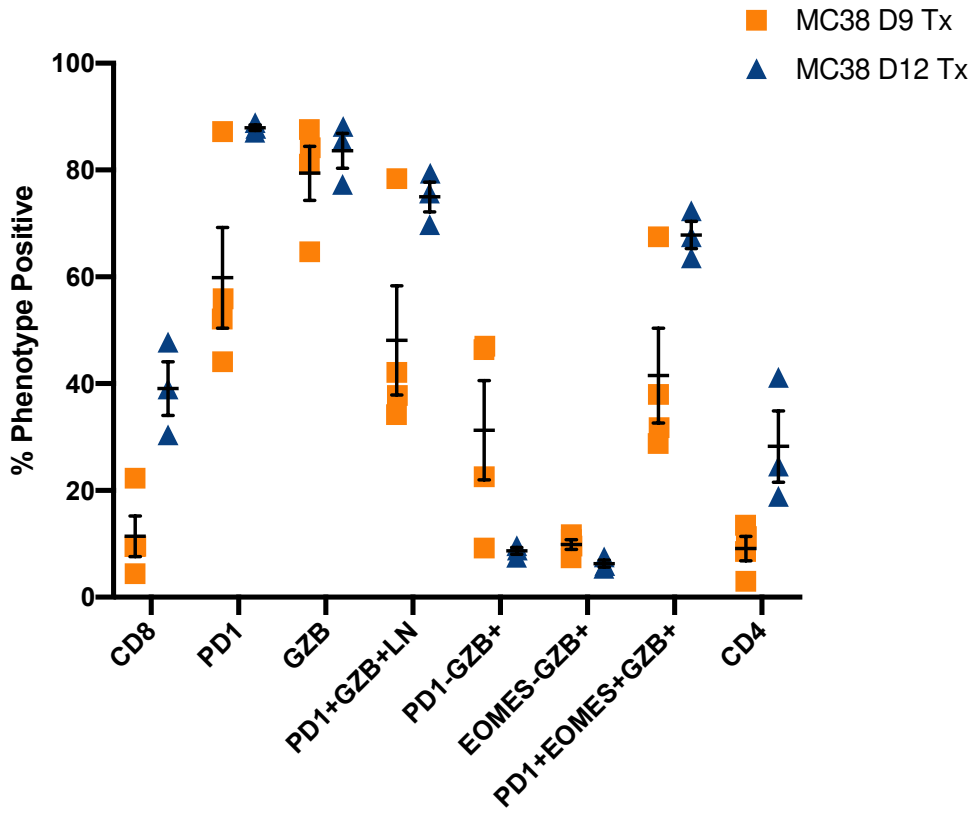

Supplemental Figure S2 – Individual tumor cellular phenotype measurements as determined by flow cytometry for anti-PD-1 and CTLA-4 treated MC38 tumors at nine (orange box) and twelve (blue triangle) days post-tumor implantation. Selected cell phenotypes as indicated on the x-axis were determined by flow cytometry using gating strategies described in the methods. Differences observed demonstrate that at 12 days post inoculation, the majority of tumors display higher levels markers of exhaustion (PD-1 and EOMES-positive) and are phenotypically distinct from day 9 tumors. Error bars represent the standard error measurement of each group (n=4).

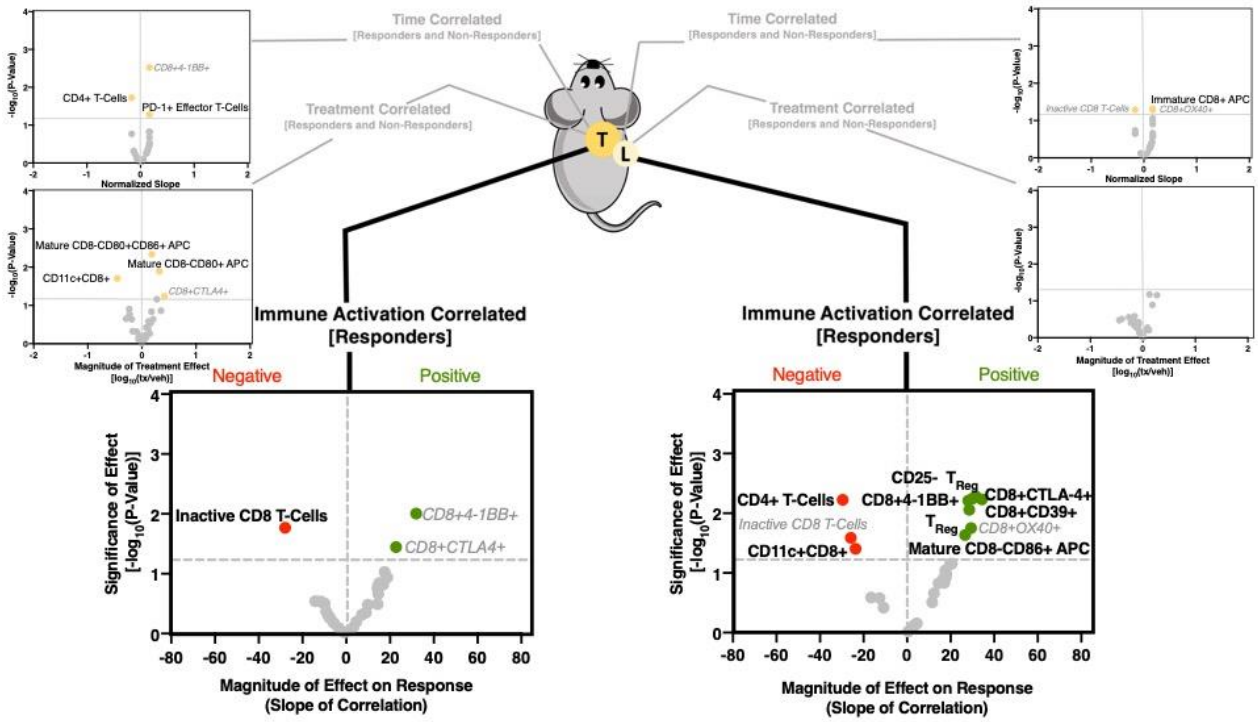

Supplemental Figure S3 - Volcano plots of the $-\log_{10}$(P-value) versus the slope (GZP PET and time) or $\log_{10}(Average_{Tx}/Average_{Veh})$ of the P value of the linear correlation between time GZP PET signal and individual cellular phenotypes quantified by flow cytometry in CT26 Tumors. P values were determined by either the probability of a non-zero slope for the linear correlation (GZP PET and time) or a two-tailed T test (treatment). Correlations found in the tumor are shown on the left, and those from the tumor draining lymph node are right. Points with a P-value less than 0.05 are labeled, yellow dots correspond to significant correlations for time and treatment, red dots correspond to negative GZP PET correlations, and green dots correspond to positive GZP PET correlations. Bolded labels indicate those that are unique to a specific correlation, gray and italicized labels indicate those that are found in multiple correlations.

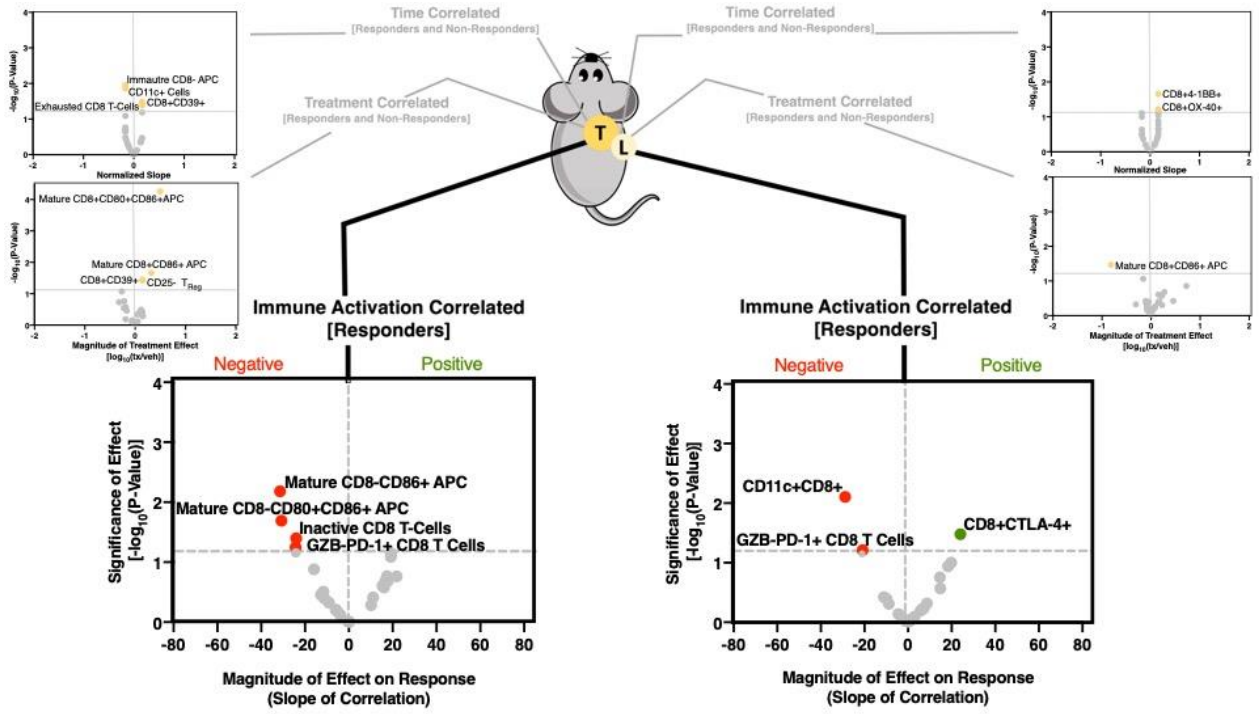

Supplementary Figure S4 - Volcano plots from MC38 tumors divided into time, treatment and immune activation (GZP PET) correlations in the same manner as CT26 tumors. Correlations found in the tumor are shown on the left, and those from the tumor draining lymph node are right. Points with a P-value less than 0.05 are labeled, yellow dots correspond to significant correlations for time and treatment, red dots correspond to negative GZP PET correlations, and green dots correspond to positive GZP PET correlations. Bolded labels indicate those that are unique to a specific correlation, gray and italicized labels indicate those that are found in multiple correlations.

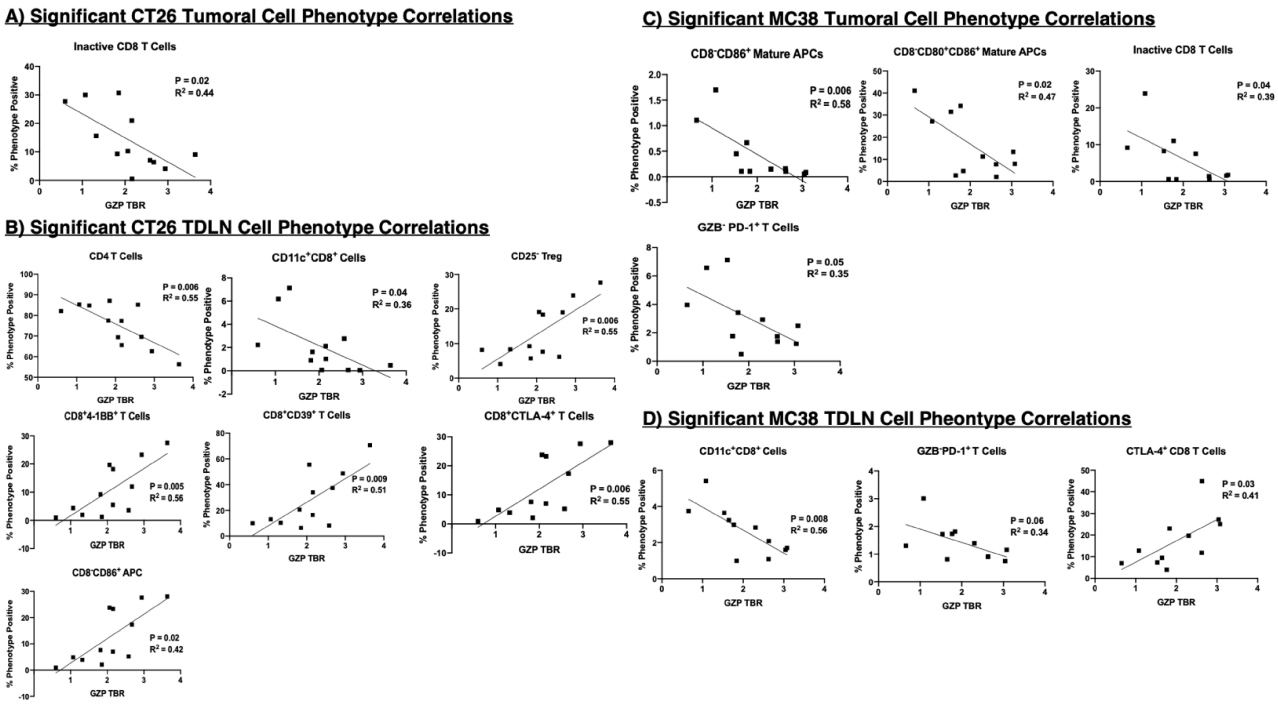

Supplemental Figure S5 – All correlations between GZP PET signal in the tumor and flow cytometry-measured cellular phenotypes found in A) CT26 tumors, B) CT26 tumor draining lymph nodes, C) MC38 tumors, and D) MC38 tumor draining lymph nodes with a statistically significant non-zero slope. Dots represent individual tumor measurements, and lines are drawn based on parametric linear regression, with the P value and R^2 for each regression displayed on the graph.

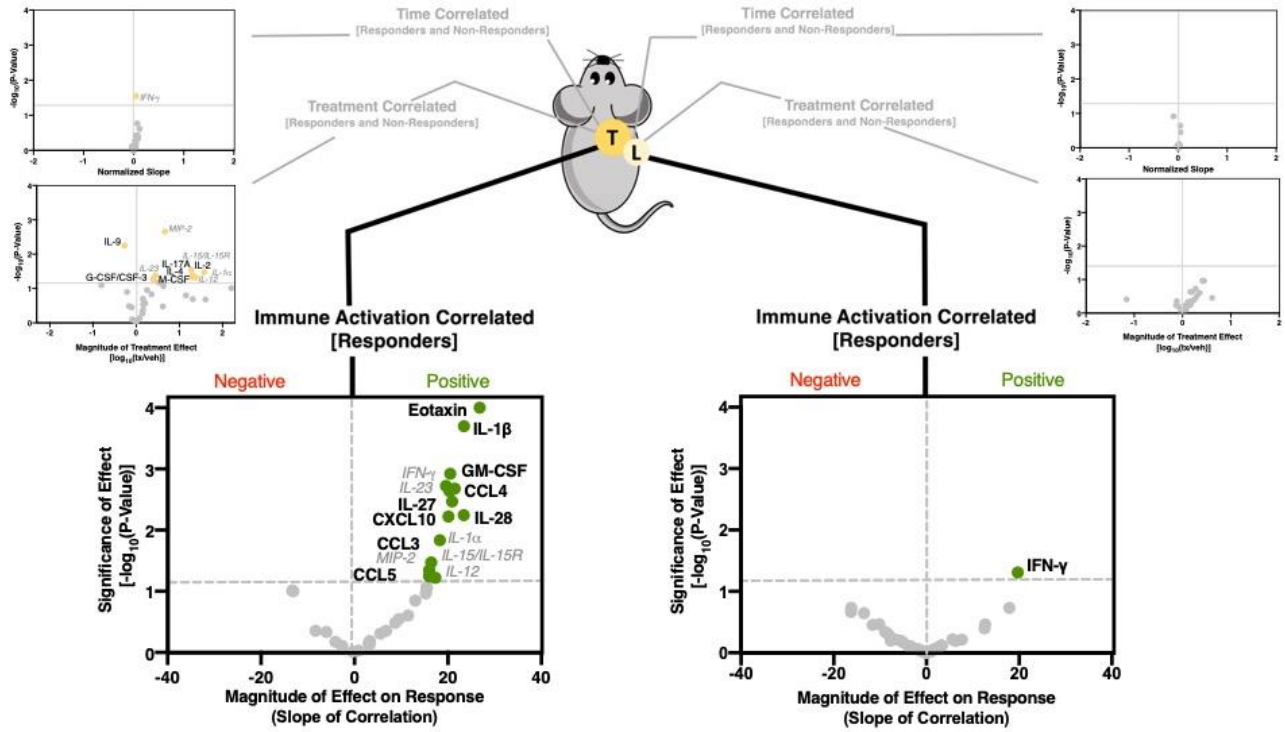

Supplementary Figure S6 - Cytokine and chemokine correlations with time, treatment and immune activation (GZP PET) from CT26 tumors. Volcano plots were generated using the same methodology as for cell phenotypes and are labeled using the same schema.

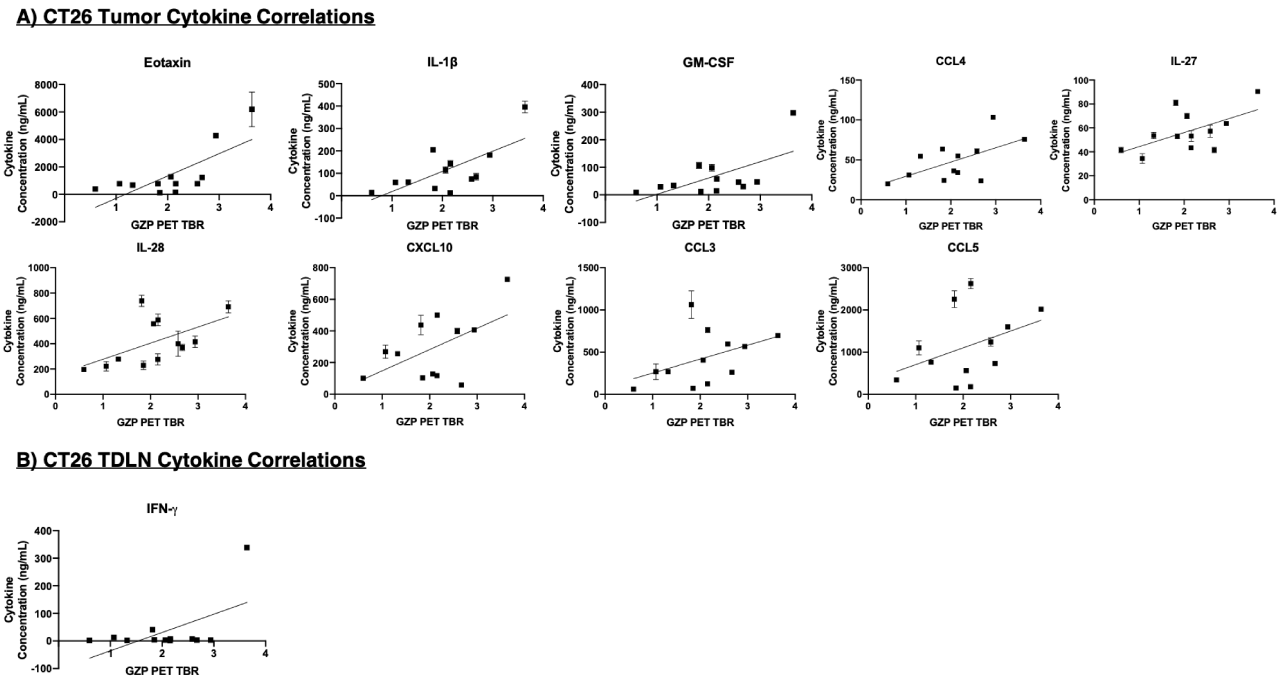

Supplemental Figure S7 – All correlations between GZP PET signal in the tumor and cytokine measurements from in A) CT26 tumors and B) CT26 tumor draining lymph nodes with a statistically significant non-zero slope. Dots represent individual tumor measurements, and lines are drawn based on parametric linear regression.

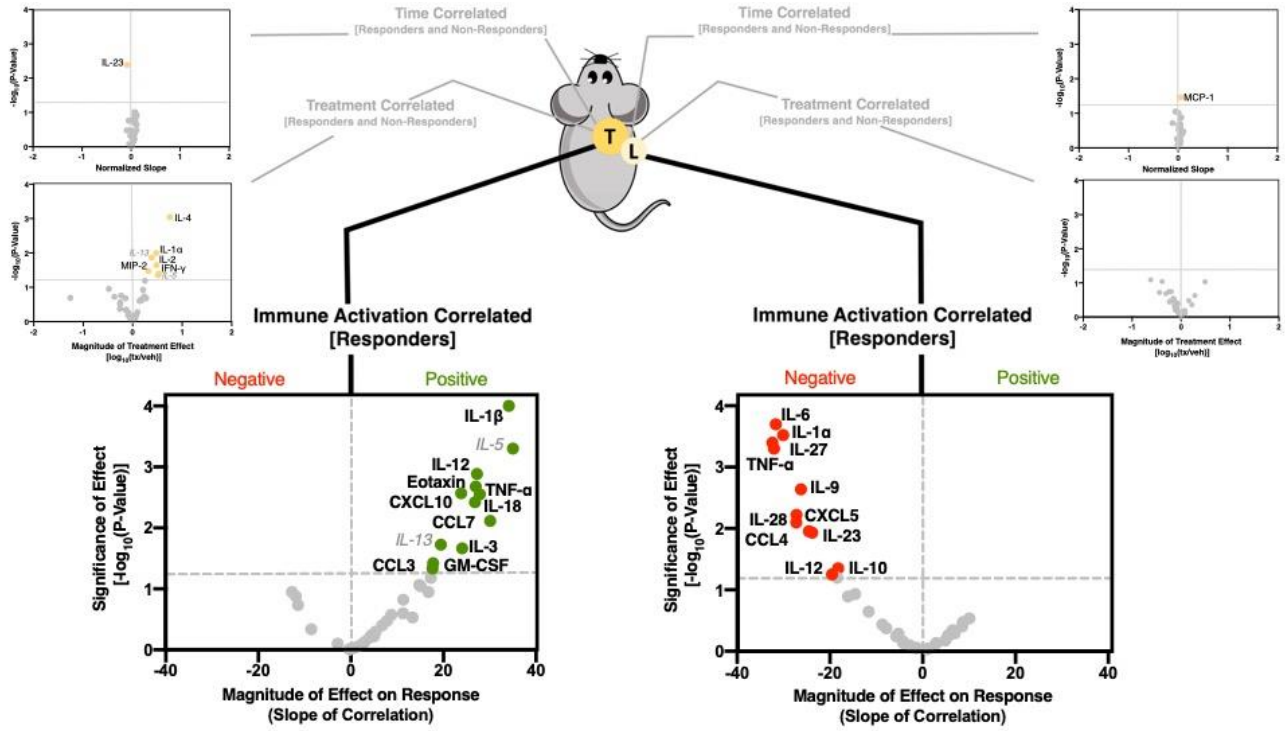

Supplementary Figure S8 - Cytokine and chemokine correlations with time, treatment and immune activation (GZP PET) from MC38 tumors. Volcano plots were generated using the same methodology as for cell phenotypes and are labeled using the same schema.

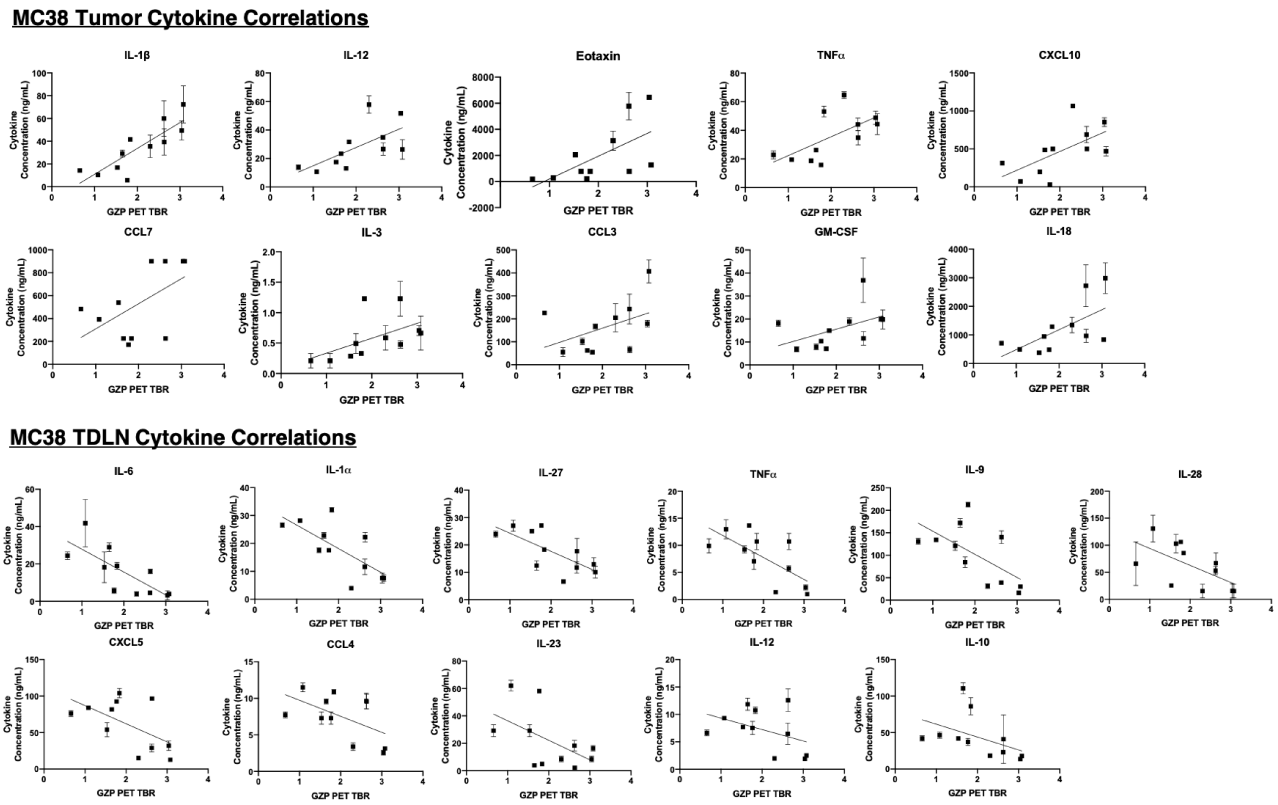

Supplemental Figure S9 – All correlations between GZP PET signal in the tumor and cytokine measurements from in A) MC38 tumors and B) MC38 tumor draining lymph nodes with a statistically significant non-zero slope. Dots represent individual tumor measurements, and lines are drawn based on parametric linear regression.